Plasma Crystal: Coulomb Crystallization in a Dusty Plasma

H. Thomas,* G. E. Morfill, and V. Demmel
Max-Planck-Institut für Extraterrestrische Physik, 85740 Garching, Germany

J. Goree†
Department of Physics and Astronomy, The University of Iowa, Iowa City, Iowa 52242

B. Feuerbacher and D. Möhlmann
DLR, Institut für Raumsimulation, 51140 Köln, Germany
(Received 25 January 1994)

A macroscopic Coulomb crystal of solid particles in a plasma has been observed. Images of a cloud of 7-μm "dust" particles, which are charged and levitated in a weakly ionized argon plasma, reveal a hexagonal crystal structure. The crystal is visible to the unaided eye. The particles are cooled by neutral gas to 310 K, and their charge is $>9800e$, corresponding to a Coulomb coupling parameter $\Gamma > 20700$. For such a large Γ value, strongly coupled plasma theory predicts that the particles should organize in a Coulomb solid, in agreement with our observations.

PACS numbers: 52.25.-b, 64.70.-p, 94.10.Nh

The search for model systems of crystalline structures to study phase transitions was initiated by Wigner in the 1930s with the theory of the Wigner crystal [1]. Since that time experimental verification has been achieved for several specific systems. On the atomic scale these are ion crystals [2–4] and electron crystals [5] and on macroscopic scales colloidal crystals in aqueous solutions [6,7]. Each of these systems has advantages and disadvantages for the detailed study of the phase transition of interest, such as formation, growth, and melting of crystalline structures.

Here we report an experimental observation of a macroscopic Coulomb crystal formed from a dusty plasma. We term this structure a "plasma crystal." Because of its macroscopic size, and the ease of photographing it and controlling it over a wide range of parameters (including plasma density, temperature, neutral gas, and particle size), the detailed study of plasma crystals could well lead to a better understanding of phase transitions. Based on theoretical calculations this was first suggested by Ikezi [8].

Dusty plasmas have been the subject of intensive study for astrophysics and plasma-aided manufacturing. In space, dusty plasmas are ubiquitous [9–11], including interstellar clouds, circumstellar and protoplanetary accretion disks, nova ejecta, and planetary magnetospheres. The thermodynamics, chemistry, and electromagnetic evolution of these systems are affected and sometimes dominated by dust. In microelectronics fabrication, particles can grow in the plasmas in surface processing reactors, and remain electrically suspended there until they fall to a surface and contaminate it [12,13]. Thus it is not surprising that astronomers and industrial researchers have investigated many physical processes [12–18] including especially the problem of dust charging [19–22].

A dust particle, like any surface exposed to a plasma, is charged by collecting ions and electrons, or by photoemission and secondary emission. In the absence of electron emission, the charging process is dominated by the incoming flux of electrons and ions from the surrounding plasma. The charge on an isolated particle in the plasma is $Q_p = C\Phi_s$, where $C = 4\pi\varepsilon_0 r$ is the capacitance, r the particle's radius, and the steady-state surface potential Φ_s is calculated by equating the ion and electron fluxes [21,22]. For nondrifting Maxwellian distribution functions characterized by ion and electron temperatures T_i and T_e, Φ_s is the solution of $[1 - (e\Phi_s/k_BT_i)] = (m_ik_BT_e/m_ek_BT_i)^{1/2}\exp(e\Phi_s/k_BT_e)$, while for drifting distributions a more general relation is satisfied [19]. These expressions are suitable for an isolated particle, but Φ_s and Q_p are diminished below this level for particles with sufficient number density n_p to deplete the electron density n_e, as will happen unless $P \ll 1$, where $P = 695T_e r n_p/n_e$, with T_e in eV and r in μm [20,22,23]. Each particle is surrounded by a Debye cloud of the opposite charge, characterized by a shielding length λ. For an infinite nondrifting plasma, λ is the "linearized" Debye length $(1/2\lambda_i^2 + 1/\lambda_e^2)^{-1/2}$ [24], where $\lambda_i \ll \lambda_e$ for a typical discharge with cold ions ($T_i \ll T_e$). According to the Bohm sheath criterion for a dust-free discharge, at the edge the ions drift at approximately $c_s = (k_BT_e/m_i)^{1/2}$, so they enter the sheath with the same energy as electrons. Accordingly λ might be modeled more accurately as $\lambda \approx \lambda_e$.

The transition from random aggregates of dust in plasmas to a more ordered structure requires special conditions. Early investigations on plasma crystallization were done in the context of one-component plasmas (OCP). In an OCP, such as a pure ion plasma, overall confinement is effected by a fixed "neutralizing background," e.g., electromagnetic fields. The thermodynamics is described by the Coulomb coupling parameter, $\Gamma = Q_p^2/4\pi\varepsilon_0 k_BT_p\Delta$, which is the ratio of the

0031-9007/94/73(5)/652(4)$06.00

interparticle Coulomb potential energy to the thermal energy. Here Δ is the interparticle distance and T_p is the particle temperature. Monte Carlo simulations [25] have predicted a solid-liquid phase transition at a critical value $\Gamma_c = 172$. For $\Gamma > \Gamma_c$ the system is a solid. In general plasmas with $\Gamma > 2$ are uncommon, and they are said to be "strongly coupled."

Unlike an OCP, a dusty plasma has a "neutralizing background" that is not fixed. The background plasma of ions and electrons adjusts self-consistently to provide Debye shielding. The thermodynamics is thus more complicated than for OCPs. Borrowing from colloidal suspension theory, Farouki and Hamaguchi [26] proposed to describe the thermodynamics of the charged dust by two dimensionless parameters, Γ and the ratio $\kappa = \Delta/\lambda$. Their numerical simulations [26] showed a transition between fluid and solid phases at a critical value Γ_c, depending on the interaction range κ. Although some of the assumptions in the simulation, such as the expression for the intergrain potential energy and a small simulation box with cubic boundary conditions, may be unsuited to our experiment, the results are revealing. For a certain particle density, they indicate a value of $\Gamma_c \geq 100$ for $\kappa = 0.5$ for the liquid-solid transition.

In the present experiment we investigate the structure of a cloud of charged particles levitated in a weakly ionized plasma. A low-power argon discharge at 2.05 ± 0.05 mbar was formed by applying a 13.56-MHz signal to the lower electrode of a parallel-plate reactor (see Fig. 1). The lower electrode is a disk 8 cm in diameter, while the upper is a ring, with inner and outer diameters of 3 and 10 cm, respectively. The electrode separation is 2 cm. The dc self-bias of the lower electrode was -14.5 ± 0.5 V, measured at the electrical feedthrough. The rf power was 4.5 ± 0.2 W (forward minus reverse) measured between the rf generator and the matching network. This measurement does not account for losses in the matching network, in the connecting wires, or in the reactor hardware. These losses could be 90% or more [27]; hence we roughly estimate the power coupled to the plasma as 0.4 ± 0.3 W.

A few milligrams of 7.0 μm diameter melamine/formaldehyde spheres (± 0.2 μm size distribution) are placed in a sieve above the hole in the upper electrode. This is agitated to release particles into the plasma.

The particles were seen as a thin disk-shaped cloud, levitated above the center of the lower electrode, near the sheath-plasma boundary. Particles were organized in approximately 18 planar layers parallel to the electrode. The cloud diameter was approximately 3 cm. Observations were made by illuminating a plane with a sheet of HeNe laser light, with a thickness of 110 ± 23 μm and a breadth of 2 cm. It is adjustable to various heights above the lower electrode. Scattered light is viewed at 90° through a hole in the upper electrode. Individual particles were easily seen with the unaided eye and with a charge-coupled device video camera fitted with a macro lens. A 200-mm macro lens with extension tubes provided $\times 1$ magnification for the data shown below, while a long-distance microscope lens ($\times 13$ magnification) revealed that the particles in the plasma were either individual grains or agglomerates of two grains. The latter populated the lower lattice ≈ 6 layers of the cloud, presumably due to their greater mass to charge ratio.

Figure 2 shows an image of the particle cloud in a single plane. Note the organized structure and nearly uniform particle spacing. The image area is 7.7×7.7 mm^2 and contains 724 particles. Assuming equal particle spacing in all directions, this corresponds to $n_p = (4.3 \pm 0.2) \times 10^4$ cm^{-3}.

A numerical analysis of Fig. 2 verifies it as a "plasma crystal." We digitized the image to identify the particle locations and to describe the Voronoi (Wigner-Seitz)

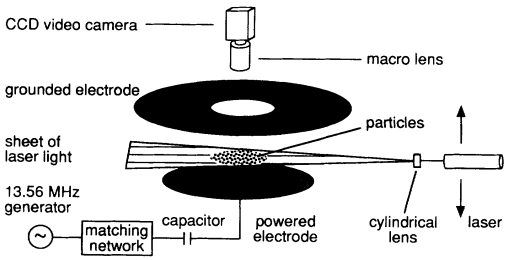

FIG. 1. Schematic of apparatus. A discharge is formed by capacitively coupled rf power applied to the lower electrode. A vacuum vessel, not shown, encloses the electrode assembly. A cylindrical lens produces a laser sheet in a horizontal plane, with an adjustable height. The dust cloud is viewed through the upper ring electrode.

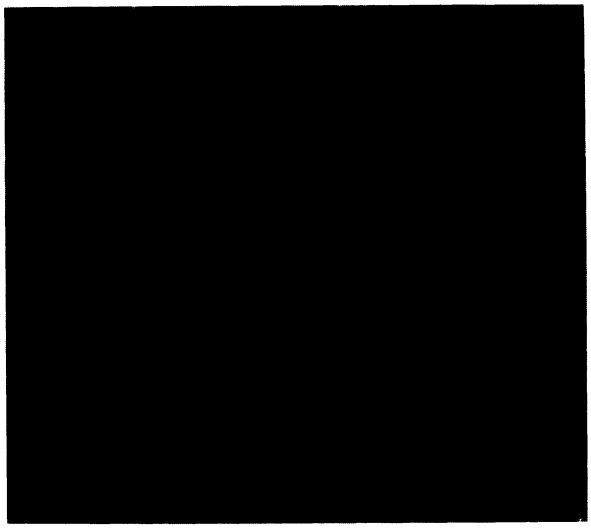

FIG. 2. Image of the particle cloud in a plane above the lower electrode. The area shown is 7.7×7.7 mm^2 and contains 724 particles of 7-μm diameter.

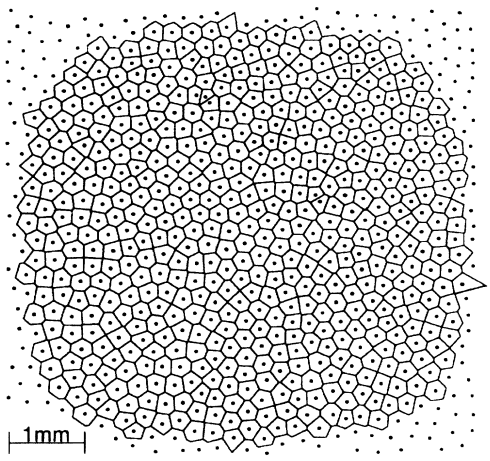

FIG. 3. Voronoi analysis of particle locations from the image shown in Fig. 2.

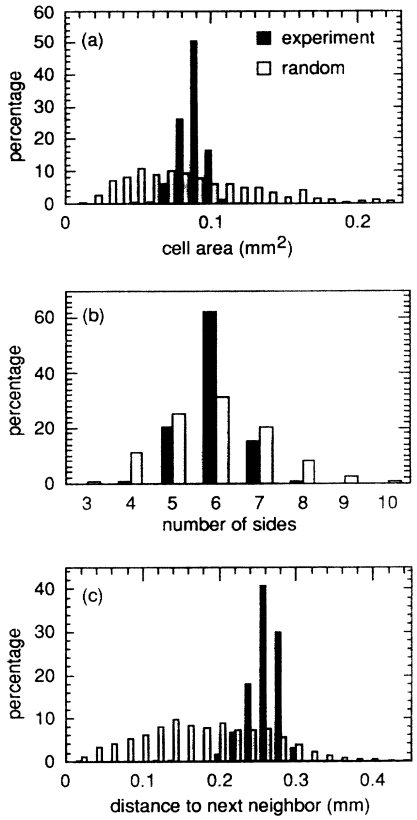

FIG. 4. Distribution of (a) Voronoi-cell areas, (b) number of Voronoi-cell sides, and (c) near-neighbor distances. The experimental data (black columns) are from the image in Fig. 2. Data for a random-point distribution (white columns) is shown for comparison.

cells (see Fig. 3). The cells are mainly six sided, with nearly equal areas and uniform spacing, as shown in Fig. 4. The mean interparticle distance Δ (lattice constant) is 250 μm. The measurements were compared with a synthetic random particle distribution using the same properties—number and density—as in the experiment. This simulates a dusty plasma in its "gas phase." The comparison is shown in Fig. 4. It is obvious that the observed particle structure is more crystalline than gaslike. The video showed the individual particles oscillating gently about fixed equilibrium centers in what appeared to be Brownian motion. Occasionally a grain diffused through the structure, visibly perturbing the positions of the nearest particles.

In order to estimate the coupling parameter Γ we need to know the particles' kinetic energy (or temperature) and charge. The particles are cooled by the neutral gas. Based on frame-by-frame measurements of the mean particle velocity, we estimate the particle kinetic temperature to $T_p = 310$ K, which is close to room temperature. A comparable temperature was measured by Boufendi *et al.* [13] using laser-Doppler velocimetery; their particle size and Γ were much smaller than ours.

We estimate the plasma parameters and the grain charge in the following way. We assume room temperature ions and other parameters that are typical [27] of low-power rf discharges: $k_B T_e = 3 \pm 1$ eV, and plasma density $n_i = 10^9$ cm^{-3}, accurate to a factor of 4. (In this experiment, we did not measure any of these parameters.) We calculated the potential Φ_s for two extreme cases of the ion drift speed, zero and c_s, as discussed above. Correspondingly, we find $(-7.2 \pm 2.0\ \text{V}) \geq \Phi_s \geq (-11.7 \pm 3.9\ \text{V})$ for an isolated grain. For our discharge the parameter P lies in the range $0.08 \leq P \leq 1.2$, where the uncertainty arises from the uncertainty of n_i. Correspondingly, the charge is reduced by 6% to 44% from the isolated particle case [20,22]. Using these values, we estimate the grain charge to lie between the extreme values $-9800 \geq Q_p/e \geq -27\,300$. The shielding length is estimated to lie between the "linearized" Debye length and λ_e, $52 \leq \lambda \leq 405$ μm, resulting in $4.8 \geq \kappa \geq 0.6$. The Coulomb coupling parameter Γ is then estimated to be $> 20\,700$. Our observation of a crystalline structure is consistent with this large value of Γ.

The crystal forms easily at these parameters, because the large charge assures strong interparticle Coulomb forces, while the neutral gas cools the particles to a low temperature. When the rf power was raised, however, we found that particles moved more violently, and many appeared to have no equilibrium positions, so the cloud qualitatively appeared to be liquidlike. However, we did not observe a distinct phase transition of the cloud as a whole. One problem in observing a phase transition is that we view only a single two-dimensional layer, and a change of the plasma conditions (e.g., heating the cloud by increasing the rf power) leads to a displacement of

the layers in the cloud perpendicular to the plane of observation.

While the suspension of colloidal crystals is affected by buoyancy in electrolyte experiments [4,5], in our case we must rely on electrostatic forces to balance gravity and ion drag [28]. The electrostatic levitation arises from a sheath electric field due to the negative dc self-bias on the lower electrode. (The grains cannot respond to the fast 13 MHz fields that are also present.) Positive ions flowing toward the lower electrode exert the ion drag force. The thermophoretic force [29], due to a gas temperature gradient, is negligible for the conditions relevant to Figs. 2–4. Measurements showed that the electrode temperature was not elevated above the surroundings. In addition to these forces, there are interparticle electrostatic forces, which are responsible for the internal structure of the cloud, including the crystalline structure. The strong gravitational field at the Earth's surface restricts the formation of a "plasma crystal" to a few lattice planes and may lead to inhomogeneities. Studies investigating the possibilities of microgravity are in progress [30].

In conclusion, we have shown an optical image of a two-dimensional ordered structure of a charged particle cloud in a plasma, a "plasma crystal." Image analysis reveals the crystalline structure, which is consistent with a large value of the Coulomb coupling parameter.

One of us (J. G.) was supported by NSF ECS-92-15882, NASA NAGW-3126, and NASA NAG8-292.

*Permanent address: DLR, Institut für Raumsimulation, 51140 Köln Germany. Electronic address: Hubertus.Thomas@europa.rs.kp.dlr.de

†Electronic address: john-goree@uiowa.edu

[1] E. Wigner, Trans. Faraday. Soc. **34**, 678 (1939).
[2] F. Diedrich *et al.*, Phys. Rev. Lett. **59**, 2931 (1987).
[3] S. L. Gilbert, J. J. Bollinger, and D. J. Wineland, Phys. Rev. Lett. **60**, 2022 (1988).
[4] I. Waki *et al.*, Phys. Rev. Lett. **68**, 2007 (1992).
[5] H. W. Jiang *et al.*, Phys. Rev. Lett. **65**, 633 (1990).
[6] D. H. Van Winkle and C. A. Murray, J. Chem. Phys. **89**, 3885 (1988).
[7] A. Kose *et al.*, J. Colloid. Interface Sci. **44**, 330 (1973).
[8] H. Ikezi, Phys. Fluids **29**, 1764 (1986).
[9] C. K. Goertz, Rev. Geophys. **27**, 271 (1989).
[10] E. Grün, G. E. Morfill, and D. A. Mendis, in *Planetary Rings*, edited by A. Brahic and R. Greenberg (Univ. Arizona Press, Tucson, 1984), p. 275.
[11] T. W. Hartquist, O. Havnes, and G. E. Morfill, Fundamentals Cosmic Phys. **15**, 107 (1992).
[12] G. S. Selwyn, J. E. Heidenreich, and K. L. Haller, Appl. Phys. Lett. **57**, 1876 (1990).
[13] L. Boufendi *et al.*, J. Appl. Phys. **73**, 2160 (1993).
[14] G. E. Morfill, E. Grün, and T. V. Johnson, Planetary Space Sci. **28**, 1087 (1980).
[15] C. K. Goertz and G. E. Morfill, Icarus **53**, 219 (1983).
[16] W. Pilipp *et al.*, Astrophys. J. **314**, 341 (1987).
[17] J. A. Burns, M. R. Showalter, and G. E. Morfill, in *Planetary Rings* (Ref. [10]), p. 200.
[18] G. E. Morfill, C. K. Goertz, and O. Havnes, J. Geophys. Res. **98**, 1435 (1993).
[19] E. C. Whipple, Rep. Prog. Phys. **44**, 1197 (1981).
[20] O. Havnes, T. K. Aanesen, and F. Melandsø, J. Geophys. Res. **95**, 6581 (1990).
[21] B. T. Draine and E. E. Salpeter, Astrophys. J. **231**, 77 (1979).
[22] J. Goree, Plasma Sources Sci. Technol. (to be published).
[23] G. E. Morfill, Adv. Space Res. **3**, 87 (1983).
[24] J. E. Daugherty *et al.*, J. Appl. Phys. **72**, 3934 (1992).
[25] D. H. E. Dubin, Phys. Rev. A **42**, 4972 (1990).
[26] R. T. Farouki and S. Hamaguchi, Appl. Phys. Lett. **61**, 2973 (1992).
[27] V. A. Godyak, R. B. Piejak, and B. M. Alexandrovich, Plasma Sources Sci. Technol. **1**, 36 (1992).
[28] M. D. Kilgore *et al.*, J. Appl. Phys. **73**, 7195 (1993).
[29] G. M. Jellum, J. E. Daugherty, and D. B. Graves, J. Appl. Phys. **69**, 6923 (1991).
[30] G. E. Morfill *et al.*, COLUMBUS Precursor Flights Proposal, 1991.

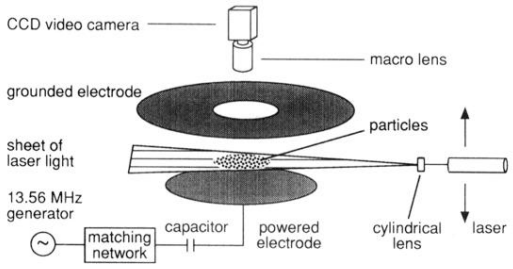

FIG. 1. Schematic of apparatus. A discharge is formed by capacitively coupled rf power applied to the lower electrode. A vacuum vessel, not shown, encloses the electrode assembly. A cylindrical lens produces a laser sheet in a horizontal plane, with an adjustable height. The dust cloud is viewed through the upper ring electrode.

FIG. 2. Image of the particle cloud in a plane above the lower electrode. The area shown is 7.7×7.7 mm^2 and contains 724 particles of 7-μm diameter.